IEEE Access
Multidisciplinary | Rapid Review | Open Access Journal

Received July 15, 2019, accepted September 6, 2019, date of publication September 19, 2019, date of current version October 10, 2019.

Digital Object Identifier 10.1109/ACCESS.2019.2942425

Geometrical Structure Classification of Target HRRP Scattering Centers Based on Dual Polarimetric H/α Features

TENG LONG[1,2], (Fellow, IEEE), LIANG ZHANG[1,2], YANG LI[1,3], AND YANHUA WANG[1,3]

[1]Radar Research Laboratory, School of Information and Electronics, Beijing Institute of Technology, Beijing 100081, China
[2]Beijing Key Laboratory of Embedded Real-Time Information Processing Technology, Beijing 100081, China
[3]Chongqing Innovation Center, Beijing Institute of Technology, Chongqing 401147, China

Corresponding author: Yang Li (bit_liyang@bit.edu.cn)

This work was supported in part by the National Natural Science Foundation of China under Grant 61701026, in part by the Chang Jiang Scholars Programme under Grant T2012122, and in part by the Youth Science and Technology Innovation Leader of National Innovation Talent Promotion Program under Grant 2013RA2034.

ABSTRACT Polarimetric high resolution range profile (HRRP) contains the geometrical structural information along radar line-of-sight and has shown great potentials in target recognition. In existing researches, H/α decomposition has been applied to exploit global polarimetric features of a single HRRP from its spatially averaged coherent matrix, which loses target local scattering information. In this paper, we propose to apply the H/α decomposition along the slow time dimension in a dual polarimetric HRRP sequence. The H and α features are extracted for each target scattering center by averaging its samples in different observations of the HRRP sequence, which provides both target local high resolution and polarimetric scattering characteristics. We also design a novel six-zone H-α plane for geometrical structure classification of target scattering centers. Simulation and experimental results show the effectiveness of the proposed method and display its good potentials for practical applications.

INDEX TERMS High resolution range profile (HRRP) sequence, dual polarization, H/α decomposition, geometrical structure classification.

I. INTRODUCTION

High resolution range profile (HRRP) represents the distribution of target scattering centers along radar line-of-sight (LOS). Because of its low requirement on the acquisition, storage and processing, it plays an important role in radar automatic target recognition [1]–[4], especially in reconnaissance, surveillance and guidance applications. Polarization, as an important intrinsic property of electromagnetic wave, reflects target physical scattering mechanisms [5]–[7]. Thus polarimetric information is generally used in conjunction with HRRP in order to enhance radar automatic target recognition performance [8]–[10].

Full polarimetric system and dual polarimetric system are the two options to obtain target polarimetric HRRP [11], [12]. Full polarimetric radar transmits two orthogonal polarizations alternatively or simultaneously and records both at the same time, thus obtaining the full polarimetric information of a target [13], [14]. Dual polarimetric radar, which transmits a single linear or circular polarization and receives two orthogonal polarizations simultaneously, obtains partial polarimetric information of a target [15]–[18]. Although full polarimetric system maximizes the target scattering information in the measurement, its hardware complexity and cost are much higher than dual polarimetric system. Thus, dual polarimetric system still has great values in practical applications at this stage.

Polarimetric decomposition technique is an effective approach to interpret target polarimetric scattering information, and has been widely used in remote sensing for target classification [19]–[21]. Among many polarimetric decomposition methods, the H/α decomposition method developed by Cloude and Pottier [22] is probably the most well-known technique and has been routinely applied for the classification of terrain and land in synthetic aperture radar (SAR) images [23]. Researchers also tried to use this useful method for polarimetric HRRP recognition. For instance, F. Berizzi *et al*. extracted the H and α parameters

The associate editor coordinating the review of this manuscript and approving it for publication was Weimin Huang.

from polarimetric range profiles of man-made targets and discussed the classification performance [24]. L. Guo *et al*. investigated the effectiveness of H and α features for aircraft HRRP recognition [25]. The above methods extract a single pair of H and α features of target HRRP by averaging all the range cells spatially. The resulting features only describe the general scattering mechanism of the whole target, but cannot depict the detailed information of local scattering centers, which may reduce the performance of features for distinguishing different targets.

In this paper, we propose a geometrical structure classification method of target scattering centers based on H/α decomposition technique using dual polarimetric HRRP sequence. Our research is based on a slant 45° dual polarimetric mode, in which a 45° linear polarization is transmitted followed by reception in orthogonal 45° and 135° polarizations simultaneously. We use this mode because it has advantage of not only low system complexity but also good recognition performance for certain typical geometrical structures [26]. In our method, the H and α features are extracted along the slow time dimension in HRRP sequence rather than conventional range dimension. This approach extracts H and α features for each scattering center combining polarimetric information with high resolution information. We also study the effect of noise on H and α features, and further design a novel six-zone H-α classification plane for classifying five typical geometrical structures. The effectiveness and application of classifying geometrical structure types of target HRRP scattering centers using this six-zone H-α plane are demonstrated via simulation and experimental results.

The reminder of this paper is organized as follows. Section II introduces the scattering center model for target polarimetric HRRP. Section III briefly reviews the conventional H/α decomposition method for HRRP data at first, and then proposes a H and α features extraction method for target scattering centers based on dual polarimetric HRRP sequence. Section IV discusses the impact of random noise on H and α features and introduces a new six-zone H-α plane for geometrical structure classification which resulted from the analytical study of random noise on the features. Section V presents experimental results using simulated and measured data. Section VI concludes the paper.

II. SCATTERING CENTER MODEL FOR POLARIMETRIC HRRP

In high frequency, scattering of a complex target is approximated to a sum of responses from local scattering sources, which are known as scattering centers [27]–[29]. Scattering centers mainly arise from discontinuous curvature or surface of target structures, such as edge and corner. Following the geometrical structure of a complex target, its scattering sources can be categorized by canonical scattering: specular scattering, double and multiple scattering, edge diffraction, traveling waves and so on [30]. Fig. 1 illustrates different scattering components of a vehicle, including specular scattering from the vehicle side planes or roof; double scattering between the vehicle body and ground, triple scattering from some special structures (e.g. rear side); edge diffraction on the straight or curved edges; traveling wave on some smooth surfaces of the vehicle body [31].

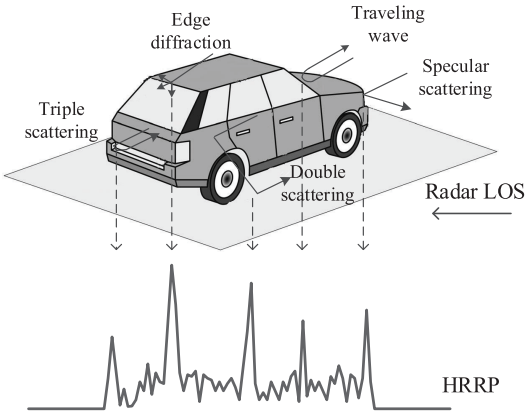

FIGURE 1. Illustration of a HRRP sample from a vehicle target, where scattering sources of vehicle geometrical structures form some scattering centers. The vehicle figure is cited from [31].

HRRP characterizes the projection of the responses from target scattering centers onto the radar LOS [32] as shown in Fig. 1. In scattering center model, HRRP can be expressed as

$$x_l(t) = \sum_{i=1}^{I} S_l^i h(t - \frac{2r_i}{c}) \exp(-j\frac{4\pi r_i}{\lambda}), \tag{1}$$

where c denotes the light speed; λ is the signal wavelength and I is the scattering center numbers; $h(t)$ represents the high resolution impulse response function after pulse compression; r_i is the radial range of i-th scattering center to the radar; S_l^i represents the complex scattering coefficient of the i-th scattering center in l polarization measurement ($l = hh, hv, vh, vv$, where h, v represent horizontally and vertically linear polarizations respectively), and S_l^i is the corresponding element of target polarization scattering matrix (PSM) in far-field, which is written as [33]

$$\mathbf{S^i} = \begin{bmatrix} S_{hh}^i & S_{hv}^i \\ S_{vh}^i & S_{vv}^i \end{bmatrix}. \tag{2}$$

It can be observed from (1) that target HRRP is seen as the combination of scattering from all scattering centers, and their scattering characteristics are described by the polarization scattering matrixes as shown in (2). Thus polarimetric HRRP has become an efficient approach to analyze the scattering information about target local details. Some geometrical models are simply utilized to describe those scattering contributions [34]–[36]. For example, a plane, a cylinder, and a sphere may represent the scattering from a plane, single curvature, and double curved surfaces, respectively; a dihedral may describe double scattering, and a trihedral may present triple scattering; a dipole may represent edge diffraction [31]. In this paper, we select five kinds of

TABLE 1. Polarization scattering matrixes and α values for typical scattering geometrical structures.

Geometrical Structure	Normalized PSM	α value (°)
Trihedral (Plane or Sphere)	$\begin{bmatrix} 1 & 0 \\ 0 & 1 \end{bmatrix}$	0
Cylinder	$\begin{bmatrix} 1 & 0 \\ 0 & 0.5 \end{bmatrix}$	18.34
Dipole	$\begin{bmatrix} 1 & 0 \\ 0 & 0 \end{bmatrix}$	45
Narrow diplane	$\begin{bmatrix} 1 & 0 \\ 0 & -0.5 \end{bmatrix}$	71.57
Dihedral	$\begin{bmatrix} 1 & 0 \\ 0 & -1 \end{bmatrix}$	90

typical geometrical models: 1) trihedral (plane or sphere); 2) cylinder; 3) dipole; 4) narrow diplane; 5) dihedral, which are commonly used to represent typical scattering types of man-made target, to characterize target scattering center types. Their normalized scattering matrixes are shown in Table 1. In the following sections, we will classify the geometrical structure types of target scattering center according to these five kinds of geometrical models based on the extracted H and α features.

III. H AND α FEATURES EXTRACTION FOR TARGET SCATTERING CENTERS

A. REVIEW OF CONVENTIONAL H/α DECOMPOSITION METHOD FOR HRRP

F. Berizzi *et al*. studied how to use H/α decomposition on full polarimetric HRRP data to extract target H and α features [24]. Under the assumption of scattering reciprocity (i.e. $S_{hv} = S_{vh}$), the PSM of each range cell can be represented as a scattering vector $\mathbf{k}$ on the Pauli's basis [37]

$$\mathbf{k} = \frac{1}{\sqrt{2}} \left[S_{hh} + S_{vv} \quad S_{hh} - S_{vv} \quad 2S_{hv} \right]^{\mathrm{T}}, \tag{3}$$

where the superscript $(\cdot)^{\mathrm{T}}$ denotes transpose operation.

The 3×3 averaged coherency matrix $\mathbf{T}$ is defined by

$$\mathbf{T} = \langle \mathbf{k}\, \mathbf{k}^{\mathrm{H}} \rangle, \tag{4}$$

where superscript $(\cdot)^{\mathrm{H}}$ is conjugate transpose, and $\langle \cdot \rangle$ means an spatial averaging operation of all range cells in a single HRRP as shown in Fig. 2. The eigenvalues and eigenvectors of averaged coherency matrix $\mathbf{T}$ can be obtained through eigendecomposition as follows

$$\mathbf{T} = \boldsymbol{U} \boldsymbol{\Lambda} \boldsymbol{U}^{-1} = \boldsymbol{U} \begin{bmatrix} \lambda_1 & 0 & 0 \\ 0 & \lambda_2 & 0 \\ 0 & 0 & \lambda_3 \end{bmatrix} \boldsymbol{U}^{-1}, \tag{5}$$

where $\boldsymbol{\Lambda}$ is a diagonal matrix containing three real eigenvalues ($\lambda_1 \geq \lambda_2 \geq \lambda_3 \geq 0$), and $\boldsymbol{U}$ is a unitary matrix containing three orthogonal eigenvectors. Each eigenvector has the following form

$$\boldsymbol{U} = \left[\boldsymbol{e_1} \quad \boldsymbol{e_2} \quad \boldsymbol{e_3} \right], \tag{6}$$

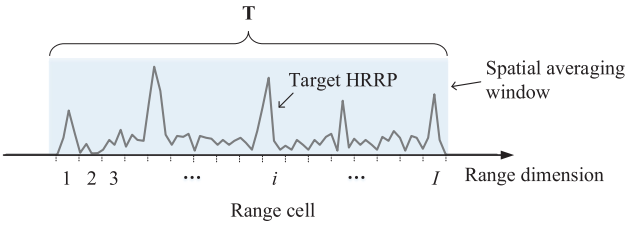

FIGURE 2. The conventional averaged coherency matrix T calculation method along the range dimension.

$$\boldsymbol{e_i} = \begin{bmatrix} e_{1i} \\ e_{2i} \\ e_{3i} \end{bmatrix} = e^{j\psi} \begin{bmatrix} \cos\alpha_i \\ \sin\alpha_i \cos\beta_i e^{i\delta_i} \\ \sin\alpha_i \cos\beta_i e^{i\gamma_i} \end{bmatrix}, \quad i = 1, 2, 3. \tag{7}$$

Then the polarimetric scattering entropy H and the polarimetric scattering angle α are defined as follows

$$H = -\sum_{i=1}^{3} p_i \log_3 p_i, \tag{8}$$

$$\alpha = -\sum_{i=1}^{3} p_i \alpha_i, \tag{9}$$

where $p_i = \lambda_i / (\lambda_1 + \lambda_2 + \lambda_3)$, $\alpha_i = \cos^{-1}(|e_{1i}|)$.

It can be seen that the H and α features are extracted from all target scattering centers [22]. Since the polarimetric status of each scattering center is commonly different as we discussed in section II, the features extracted in this way can only represent the mean scattering mechanism of the whole target, leading to the under-utilization of target detailed scattering characteristics such as the scattering property of each scattering center. This method will reduce the feature performance for classifying different targets. In order to make full use of target detailed scattering characteristics, we propose a H and α features extraction method for target scattering centers in the following subsection.

B. H AND α FEATURES EXTRACTION METHOD BASED ON DUAL POLARIMETRIC HRRP SEQUENCE

In SAR image applications, H/α decomposition method is proposed to analyze distributed targets, from which radar returns are partially polarized. It employs a statistical model which sets out with the assumption that there is always a dominant "average" scattering mechanism in each cell and then uses an eigenvalue analysis of the spatially averaged coherency matrix $\mathbf{T}$ to find the parameters of this average component [22].

In HRRP applications, a radar system generally receives a number of pulses of echoes during dwell time, and thus obtain a HRRP sequence of target [38]. For a certain target scattering center in HRRP sequence, radar returns are also partially polarized because of some unideal factors such as the presence of random noise and the fluctuation of scattering center during dwell time. Under the condition that the time series consisted of this certain target scattering center in HRRP sequence satisfies stationarity and ergodicity,

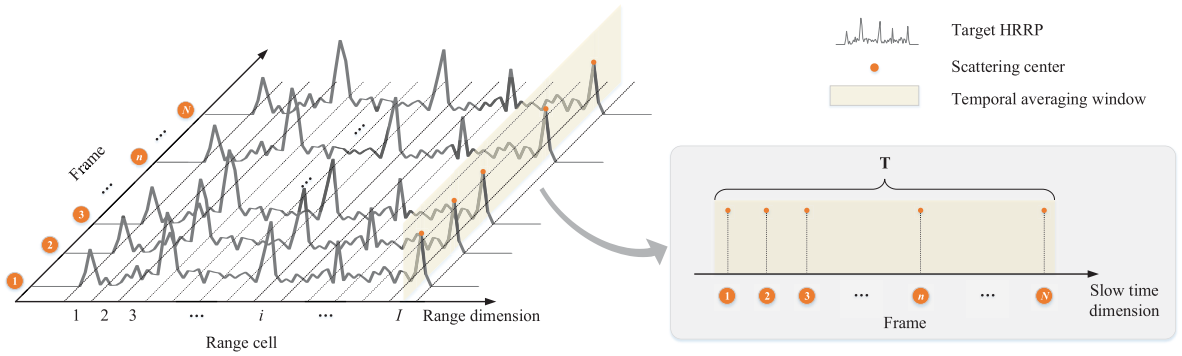

FIGURE 3. The proposed averaged coherency matrix T calculation method along the slow time dimension.

H/α decomposition method can be used in time domain to estimate the statistical parameters of this target scattering center. Thus, we propose a H and α features extraction method for target scattering centers based on dual polarimetric HRRP sequence. In the proposed method, we calculate the averaged coherency matrix $\mathbf{T}$ for each scattering center along the radar slow time dimension rather than conventional range dimension as shown in Fig. 3. In this way, original resolution of target HRRP is preserved and feature parameters are extracted for each scattering center.

In slant 45° dual polarimetric measurement mode, which transmits a 45° linear polarization and receives 45° and 135° linear polarizations, target 45° and 135° linear polarimetric HRRP sequences are used to extract H and α features for target scattering centers. Assuming that the migration of target scattering centers can be ignored relative to sampling interval in HRRP sequence, the proposed method can be summarized as the following steps:

Step 1: Obtain the measurement vector of target scattering center in slant 45° dual polarimetric mode. Under the assumption of scattering reciprocity (i.e. $S_{hv} = S_{vh}$), the measurement vector of scattering center is given by [26]

$$\mathbf{k}(n) = \frac{1}{\sqrt{2}} \begin{bmatrix} S_{hh}(n) + 2S_{hv}(n) + S_{vv}(n) \\ S_{vv}(n) - S_{hh}(n) \end{bmatrix}, \tag{10}$$

where n indicates the n-th scattering center in a sequence as shown in Fig. 3.

Step 2: Calculate the coherency matrix of target scattering center using vector $\mathbf{k}(n)$

$$\mathbf{T}(n) = \mathbf{k}(n)\,\mathbf{k}(n)^{\mathrm{H}}. \tag{11}$$

Step 3: Calculate the averaged coherency matrix $\mathbf{T}$

$$\mathbf{T} = \langle \mathbf{T}(n) \rangle_t = \frac{1}{N} \sum_{n=1}^{N} \mathbf{T}(n), \tag{12}$$

where $\langle \cdot \rangle_t$ represents the temporal averaging operation and N is the number of elements in the temporal averaging window as shown in Fig. 3. In dual polarimetric case, $\mathbf{T}$ becomes a 2×2 matrix [39].

Step 4: Perform eigenvalue decomposition of the averaged coherency matrix $\mathbf{T}$

$$\mathbf{T} = \boldsymbol{U}\boldsymbol{\Lambda}\boldsymbol{U}^{-1}. \tag{13}$$

Step 5: Extract H and α features from eigenvalues and eigenvectors

$$H = -\sum_{i=1}^{2} p_i \log_2 p_i, \tag{14}$$

$$\alpha = -\sum_{i=1}^{2} p_i \alpha_i, \tag{15}$$

where $p_i = \lambda_i/(\lambda_1 + \lambda_2)$. λ_i is the eigenvalue, and α_i is calculated from the unitary eigenvector $\boldsymbol{e_i} = e^{j\Phi_i}\left[\cos\alpha_i \;\; \sin\alpha_i e^{i\delta_i}\right]^{\mathrm{T}}$, $i = 1, 2$.

In this method, all elements in temporal averaging window as shown in Fig. 3 have the same dominant scattering property because they come from the multiple independent repeat observations of the same target scattering center. Therefore, the feature parameters extracted in this way are efficient in describing the properties of target scattering centers, which allows subsequent scattering analysis for a scattering center based on H and α features. Accordingly, it should also be ensured that the scattering centers are aligned along the time dimension in HRRP sequence and target HRRP will not fluctuate significantly during processing period. Otherwise, it may cause the deviation in scattering analysis of scattering centers based on the extracted features.

C. INTERPRETATION OF H AND α FEATURES IN SLANT 45° DUAL POLARIMETRIC MODE

The polarimetric scattering angle α, whose value range within the interval [0°, 90°], is a key parameter used for physical characteristics classification because its value is bound up with the basic scattering mechanisms of scatterers. To illustrate the mapping relations between feature α and typical scattering geometrical structures under the slant 45° dual polarimetric mode, we calculate the α values of the five typical scattering geometrical structures, which are introduced in section II. The results are listed in column 3 of Table 1.

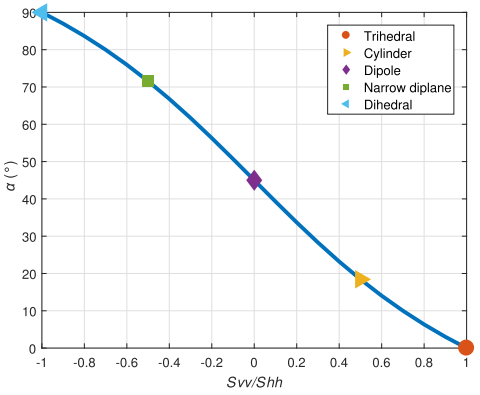

FIGURE 4. The α values of different scattering cases.

It can be seen that these typical geometrical structures are corresponding to different α values respectively.

To further explore the specific correlation of feature α value and target scattering property, we consider a general normalized canonical form diagonal scattering matrix of symmetric scatterer [40]

$$\bar{\mathbf{S}} = \begin{bmatrix} 1 & 0 \\ 0 & S_{vv}/S_{hh} \end{bmatrix}, \tag{16}$$

and calculate feature α from scattering matrix $\bar{\mathbf{S}}$ considered with S_{vv}/S_{hh} continuous variation from –1 to 1 using the proposed method. The results are shown in Fig. 4. It can be seen that α is a smoothly decreasing function of S_{vv}/S_{hh}, as the S_{vv}/S_{hh} increases so the α approaches 0°. This results indicate that valid range of feature α corresponds to a continuous change of target scattering properties as well as scattering geometrical structures. As the α changes from 0° to 90°, corresponding geometrical structure starts from the trihedral (plane or sphere, $\alpha \rightarrow 0°$), and goes through the cylinder ($\alpha \rightarrow 18.34°$) to the horizontal diplane ($\alpha \rightarrow 45°$). Then it passes narrow diplane ($\alpha \rightarrow 71.56°$) and finally changes into dihedral ($\alpha \rightarrow 90°$). Thus, feature α gives information on the target scattering property, and is useful for geometrical structure classification.

The value range of scattering entropy H is [0, 1]. In application of polarimetric SAR data classification, H describes the statistical randomness of target scattering characteristics in spatial averaging window [22]. This randomness is generally effected by two factors: the complexity of scattering types and the strength of noise. For example, the theoretical noise-free H value of a definite scatterer is zero, and it of a true noise or a completely depolarized signal or is one. In our method, the elements used for feature extraction in temporal averaging window have the same scattering property as we discussed in the previous subsection. Thus, the scattering type is pure in temporal averaging window proposed in our method and it will no longer be the factor that affects the value of H. The noise becomes the only factor which influences H value and this effect will be discussed in detail in the next section.

IV. GEOMETRICAL STRUCTURE CLASSIFICATION OF SCATTERING CENTER USING H AND α FEATURES

In this section, we discuss the effect of random noise on H and α features. Based on the comprehensive analysis and results, we propose a redesigned six-zone H-α classification plane in order to classify different geometrical structures of target scattering centers effectively and accurately even in the presence of random noise.

A. THE EFFECT OF NOISE ON H AND α FEATURES

Practical high resolution radar data often contains noise which arises from random thermal noise in the radar system's receiver. The random noise has great influences on the quality of HRRP, especially for the weak scattering centers. In this part, we focus on discussing the effect of white noise on H and α features and its impact on geometrical structure classification using the H-α plane, which is a useful tool for target classification [22], [41].

Assuming that radar measured data contains target echo signal and white Gaussian noise, the time-domain measured data $X(t)$ can be expressed as

$$X(t) = S(t) + N(t), \tag{17}$$

where $S(t)$ and $N(t)$ represent target echo signal and white Gaussian noise, respectively. Here we define the signal-to-noise ratio (SNR) for a target measured in the slant 45° dual polarimetric mode as follows

$$\text{SNR} = 10\log_{10}(\frac{E}{\sigma_1^2}), \tag{18}$$

where E is target echo signal power in 45° linear polarization receiving channel and σ_1 is the standard deviation of white Gaussian noise.

In order to investigate the effect of such noise on H and α features, white Gaussian noise is added to the slant 45° dual polarimetric scattering vectors for the five typical scattering geometrical structures which are considered in section II. A total of 5000 Monte Carlo simulations are performed for each of different SNR values (within the range 0-30dB with 2dB step). The H and α features for each target case are extracted using the proposed method, where the parameter N is set to 30 in (13). Fig. 5 plots the feature distribution clusters for each target case, and the mean center of each cluster is also marked in the figure, where "●", "▶", "◆", "■" and "◀" indicate the mean centers of trihedral, cylinder, dipole, narrow diplane and dihedral case, respectively.

From the results, it can be seen that the noise increases the polarimetric scattering entropy H values, as the SNR decreases so the entropy approaches unity (i.e., a complete random noise process). In addition, as SNR reduces, polarimetric scattering angle α gradually approaches to 45° in either target case. The standard deviation of each feature distribution cluster also increases as SNR decreases. This phenomenon infers that the geometrical structure classification performance of H-α plane gets worse with the decrease in SNR. In the effective area of H-α plane, the valid range of α

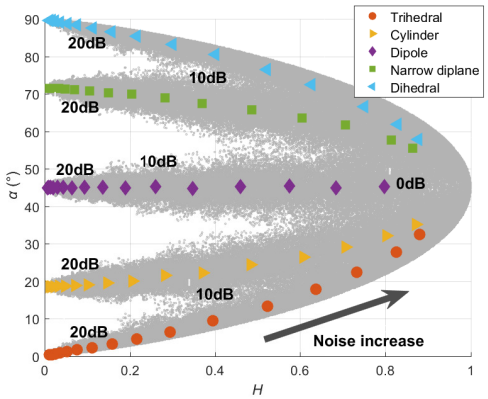

FIGURE 5. **(H, α) feature distributions of five typical geometrical structures for SNR = 0 to 30dB in 2dB increments.**

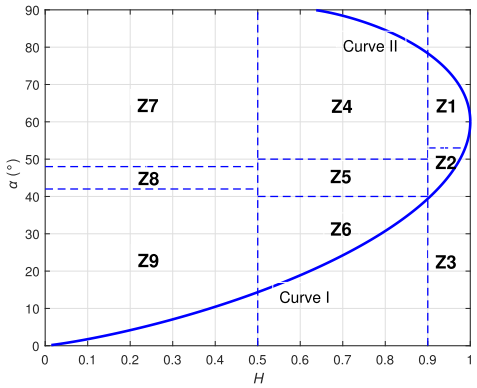

FIGURE 6. **Original H-α feature classification plane [22].**

is decreasing as the H increases, which implies a increasing inability to distinguish two adjacent geometrical structures. In particular, when $H = 0$, α could be any value between interval $[0°, 90°]$, which means that the geometrical structure type of this certain scattering mechanism could be judged by α value accurately. However, when $H = 1$, α can only be 45°, indicating that the scattering is caused by random noise and becomes complete depolarization. In this case, effective polarimetric information goes zero and feature α becomes invalid for classification.

B. A REDESIGNED SIX-ZONE H-α PLANE FOR GEOMETRIC STRUCTURE CLASSIFICATION

The H-α plane proposed by Cloude and Pottier [22] is a well-known classical unsupervised classification method. The original H-α classification plane, which is shown in Fig. 6, is divided into nine zones and the data can be classified to different scattering mechanisms according to its location on the plane. However, if this nine-zone H-α classification plane is used for geometrical structure classification in our application, the same target type will stride across several different zones which will obviously cause target classification ambiguity as we discussed above. Thus the classification zones of H-α plane should be redesigned in order to be

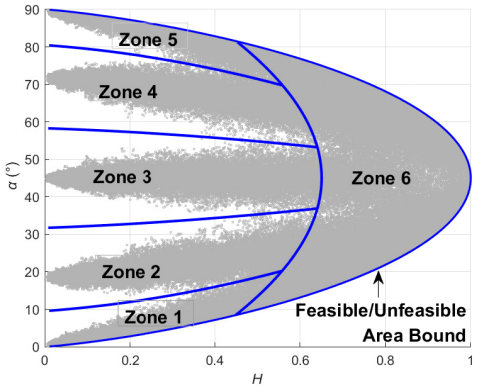

FIGURE 7. **Redesigned six-zone H-α plane for geometrical structure classification.**

effective in classifying different geometric structures due to the presence of random noise in our application.

Combining the analysis of H and α features in the previous subsection, we know that the presence of random noise shifts the feature distribution toward the region where noise is located. Thus the five banded H-α structures shown in Fig. 5 motivate the development of a redesigned H-α plane so that the five types of typical geometrical structures: trihedral, cylinder, dipole, narrow diplane, dihedral, can be more effectively and accurately classified even in the presence of random noise.

Specifically, the redesigned H-α plane is shown in Fig. 7. Not all regions are feasible in H-α plane. The boundary curve between feasible and unfeasible regions in the plane is determined by the extreme distribution of the coherence matrix $\mathbf{T}$. In dual polarimetric case, the boundary curves are defined in the following form [42]

$$\mathbf{T_1} = \begin{bmatrix} 1 & 0 \\ 0 & m \end{bmatrix}, \quad \text{and}$$
$$\mathbf{T_2} = \begin{bmatrix} m & 0 \\ 0 & 1 \end{bmatrix}, \quad 0 \le m \le 1. \tag{19}$$

Further, the feasible region is divided into six target classification zones numbered from 1 to 6 as shown in Fig. 7. Zones 1-5 are located on the left side of the plane corresponding to trihedral, cylinder, horizontal dipole, narrow diplane and dihedral, respectively. They are separated by four boundary curves which are determined by the middle α value of two adjacent geometrical structures for different SNR cases. A fitted conic is adopted for setting the bound of zone 6 and the other five zones, because low SNR may cause the misclassification of target types by H-α plane. Consequently, the region on the right side of the bound is zone 6, which corresponds to the scattering points with highly noise so that cannot be classified to a certain geometrical structure type.

V. RESULTS

In this section, we test the proposed geometrical structure classification method using the simulated data of five structure models and real data of both corner reflectors and volume

TABLE 2. Model diagrams and simulated dual polarimetric HRRPs of typical geometrical structures.

	Trihedral	Cylinder	Dipole	Narrow diplane	Dihedral
Model	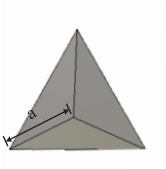	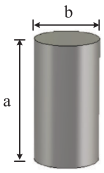	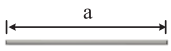	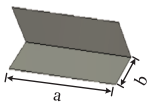	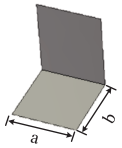
Parameter	a = 20cm	a = 20cm; b = 10cm	a = 20cm	a = 20cm; b = 10cm	a = 20cm; b = 20cm
Dual Polarimetric HRRP	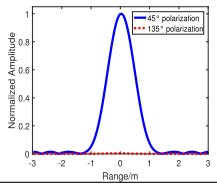	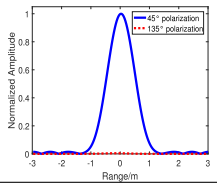	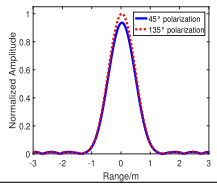	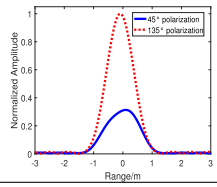	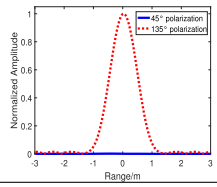

TABLE 3. Configurations for target HRRP simulation.

Parameter	Value	Parameter	Value
Center Frequency	94GHz	Bandwidth	500MHz
Azimuth	0°	Elevation	30°
Transmitting Polarization	45° linear	Receiving Polarization	45°/135° linear

targets. In our experiment, peak points of HRRP are picked as target scattering centers for analysis, and the parameter N in (13) is set to 30 in feature extraction algorithm.

A. SIMULATION RESULTS

In this part, we verify the effectiveness of the proposed method using the simulated data of the five typical geometrical structures. These simulations are conducted using a commercial electromagnetic simulation software, Computer Simulation Technology (CST). The model diagrams and dimension parameters are shown in the first and second row of Table 2 respectively. Target simulated HRRP data are computed according to the configurations given in Table 3 and shown in the third row of Table 2. For each geometrical structure, we generated three sets of HRRP sequences by adding white Gaussian noise for three different SNRs (SNR = 10, 15 and 30dB) using Monte Carlo method.

Fig. 8 shows the classification results of each target scattering center under different SNR conditions. The extracted H and α features for each case are plotted on the new six-zone classification plane and the original nine-zone classification plane for comparison. Fig. 8(b) exhibits that the H-α distributions of different geometrical structures, such as trihedral and cylinder, may locate in the same zone. It means that this original nine-zone plane shown in Fig. 6 will cause target classification ambiguity, and thus it does not apply to geometrical structures classification application. However, from Fig. 8(a), it can be seen that each scattering center is

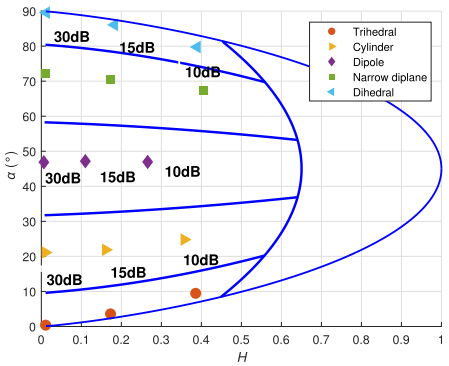

(a)

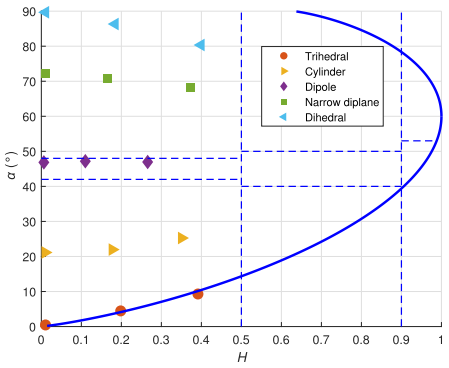

(b)

FIGURE 8. Classification results of five simulated typical geometric structures in SNR = 10, 15 and 30dB. (a) Classification using the proposed six-zone plane; (b) Classification using the original nine-zone plane.

classified to the right class type using the proposed H-α classification plane in the different SNR conditions. The locations of these feature pots extracted under three different SNR conditions are also well consistent with the previous analysis in section III, which validates the effectiveness and accuracy of the proposed method.

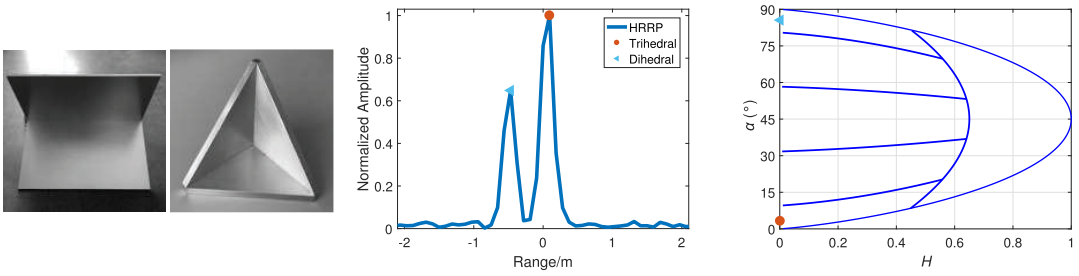

FIGURE 9. Geometrical structure classification of corner reflectors scattering centers. (a) Photographs; (b) and (c) Classification results.

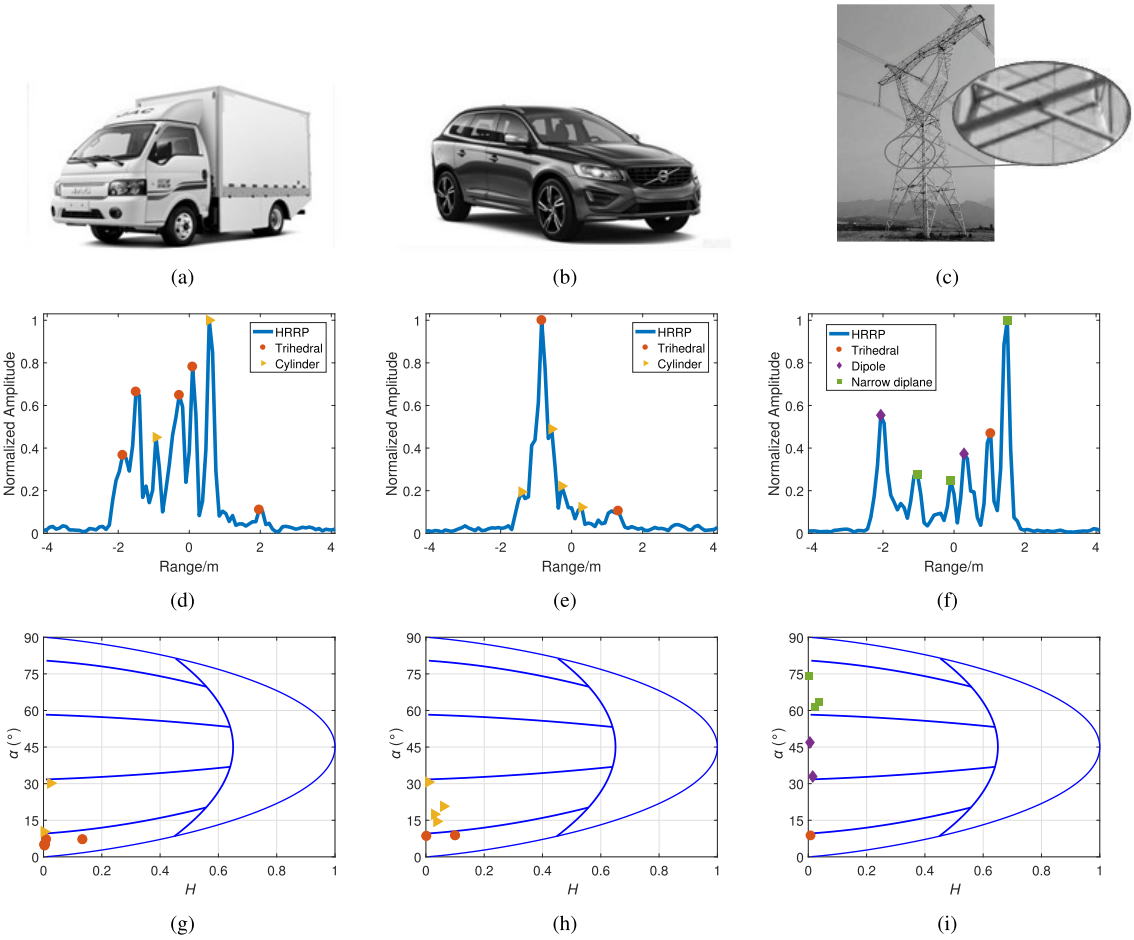

FIGURE 10. Geometrical structure classification of volume targets scattering centers: the first column (a)(d)(g), van classification result; the second column (b)(e)(h), car classification result; the third column (c)(f)(i), transmission tower classification result.

B. EXPERIMENTAL RESULTS

This part presents measurement examples of common man-made targets in practice. The experiments are divided into two parts. In the first part, two typical geometrical structures: a dihedral and a trihedral corner reflector, are measured to validate the effectiveness of the proposed method. In the second part, three complex volume targets are measured outfield, including two civilian vehicles and a man-made building. All the experimental data are collected by a dual polarimetric wideband high resolution radar, which transmits a 45° linear polarization and receives 45° and 135° orthogonal polarizations simultaneously. The polarization isolation of the two polarimetric receiving channels is higher than 25dB. The radar system operates at W-band and uses stepped-frequency linear frequency modulated signal with a synthetic bandwidth of 1250MHz. In the acquired HRRP sequence data, frame rate is over 100 frames per second. In addition, the sum power HRRP of two polarimetric receiving channels is used for display for simplicity and clarity in the following part.

1) EXPERIMENTAL RESULTS ON CORNER REFLECTORS

A trihedral and a dihedral corner reflector are measured outfield, where the dihedral corner reflector is set up in front of the trihedral corner reflector for 0.5 meter along the radar LOS direction. The photographs of the two corner reflectors are shown in Fig. 9(a).

Fig. 9(b) and (c) show the geometrical structure classification results of their scattering centers. It can be observed from Fig. 9(c) that the two feature plots are located in zone 1 and zone 5 of the redesigned six-zone H-α classification plane, indicating a trihedral and a dihedral structure respectively. The results validate that the geometrical structure types of corner reflector scattering centers are well classified using the proposed method as expected.

2) EXPERIMENTAL RESULTS ON VOLUME TARGETS

In this part, two common civilian vehicles: a van and a car, and a man-made building: a transmission tower, are measured outfield to verify the applicability of the proposed method for man-made volume target. The photographs of these three volume targets are shown in Fig. 10(a), (b) and (c), respectively. In the experiment, radar LOS points to the front of the vehicles with incident elevation angle about 10°, and the actual geometric structures of HRRP scattering centers can be known based on the distance of target geometry relative to the radar. Fig. 10(d)-(i) show the geometrical structure classification results of target scattering centers.

From Fig. 10(g) and (h), it can be seen that the scattering centers of vehicle targets are classified to trihedral and cylinder types. This result is probably caused by the specular scattering and single curvature surface scattering of vehicle body. For a further comparison between the two vehicles, it can be observed from Fig. 10(a) that van body consists of a large number of surface plate structures, and thus its most scattering centers present specular scattering and are classified to trihedral (plane) type. Unlike it, most scattering centers of the car are classified to cylinder type because its body surface are mainly smooth curved surface structures as seen in Fig. 10(b), which present single curvature surface scattering.

From Fig. 10(i), it can be seen that the scattering centers of transmission tower are mainly classified to dipole and narrow dihedral types, which represent double scattering and edge diffraction respectively. This can be explained by the fact that the transmission tower is composed of plenty of metal narrow dihedral structures which can be seen in Fig. 10(c). Double scattering occurs between the two planes and edge diffraction occurs on the straight edges on the back of narrow dihedral structures. In addition, there is also a scattering center being classified to trihedral type. This is probably because the scattering center arises from the joint of metal brackets, whose scattering presents as a trihedral scattering.

The experiment on the real data demonstrates the effectiveness and feasibility of the proposed method to classifying structural types of volume target scattering centers in practice, and the results also indicate good potentials of the proposed method in application of recognition for different targets.

VI. CONCLUSION

In this paper, we propose a geometrical structure classification method for target scattering centers based on dual polarimetric HRRP sequence. In the proposed method, the H and α features of target scattering centers are extracted along the slow time dimension in the sequence, and a six-zone H-α classification plane is designed for classifying five typical geometrical structures effectively even in the presence of random noise. The proposed method is validated using both simulated and measured data. The results demonstrate the effectiveness and accuracy of the proposed method, and also indicate its good potentials in application of radar automatic target recognition.

REFERENCES

[1] H. W. Liu, B. Feng, B. Chen, and L. Du, "Radar high-resolution range profiles target recognition based on stable dictionary learning," *IET Radar Sonar Navig.*, vol. 10, no. 2, pp. 228–237, Sep. 2015.

[2] L. Du, H. He, L. Zhao, and P. Wang, "Noise robust radar HRRP target recognition based on scatterer matching algorithm," *IEEE Sensors J.*, vol. 16, no. 6, pp. 1743–1753, Mar. 2016.

[3] D. Zhou, "Radar target HRRP recognition based on reconstructive and discriminative dictionary learning," *Signal Process*, vol. 126, pp. 52–64, Sep. 2016.

[4] J. Liu, N. Fang, Y. J. Xie, and B. F. Wang, "Scale-space theory-based multi-scale features for aircraft classification using HRRP," *Electron. Lett.*, vol. 52, no. 6, pp. 475–477, Mar. 2016.

[5] S. R. Cloude, *Polarisation: Applications in Remote Sensing*, 1st ed. New York, NY, USA: Oxford Univ. Press, 2010.

[6] J. N. Wu, Y. Chen, D. Dai, S. Chen, and X. Wang, "Clustering-based geometrical structure retrieval of man-made target in SAR images," *IEEE Geosci. Remote Sens. Lett.*, vol. 14, no. 3, pp. 279–283, Mar. 2017.

[7] M. A. Saville, J. A. Jackson, and D. F. Fuller, "Rethinking vehicle classification with wide-angle polarimetric SAR," *IEEE Aerosp. Electron. Syst. Mag.*, vol. 29, no. 1, pp. 41–49, Jan. 2014.

[8] L. Cantini, F. Berizzi, M. Martorella, and D. Calugi, "Target feature extraction in fully polarimetric high range resolution radar," in *Proc. IRS*, Krakow, Poland, May 2006, pp. 1–4.

[9] Q. Wei, C. Jian-jun, Z. Hong-zhong, and Z. Feng, "Target decomposition for fully polarimetric wideband radar system," in *Proc. IEEE ICSP*, Beijing, China, Oct. 2010, pp. 2246–2249.

[10] W. Xuesong, "Status and prospects of radar polarimetry techniques," *J. Radars*, vol. 5, no. 2, pp. 119–131, Apr. 2016.

[11] P. A. Ingwersen and W. Z. Lemnios, "Radars for ballistic missile defense research," *Lincoln Lab. J.*, vol. 12, no. 2, pp. 245–266, Feb. 2000.

[12] D. H. Dai, B. Liao, S. P. Xiao, and X. S. Wang, "Advancements on radar polarization information acquisition and processing," *J. Radars*, vol. 5, no. 2, pp. 143–155, Apr. 2016.

[13] L. Shengqi, Z. Ronghui, W. Wei, Z. Qinglin, and Z. Jun, "Full-polarization HRRP recognition based on joint sparse representation," in *Proc. IEEE Radar Conf.*, Johannesburg, South Africa, Oct. 2015, pp. 333–338.

[14] Q. Wu, F. Zhao, X. Ai, X. Ai, J. Liu, and S. Xiao, "Compressive-sensing-based simultaneous polarimetric HRRP reconstruction with random OFDM pair radar signal," *IEEE Access*, vol. 6, pp. 37837–37849, 2018.

[15] V. Chandrasekar, J. Hubbert, and V. N. Bringi, "Analysis and interpretation of dual-polarized radar measurements at +45° and –45° linear polarization states," *J. Atmos. Ocean. Technol.*, vol. 11, no. 2, pp. 323–336, Apr. 1994.

[16] J.-C. Souyris, P. Imbo, R. Fjortoft, S. Mingot, and J.-S. Lee, "Compact polarimetry based on symmetry properties of geophysical media: The $\pi/4$ mode," *IEEE Trans. Geosci. Remote Sens.*, vol. 43, no. 3, pp. 634–646, Mar. 2005.

[17] N. Stacy and M. Preiss, "Compact polarimetric analysis of X-band SAR data," in *Proc. EUSAR*, Dresden, Germany, May 2006, pp. 1–4.

[18] R. K. Raney, "Hybrid-polarity SAR architecture," *IEEE Trans. Geosci. Remote Sens.*, vol. 45, no. 11, pp. 3397–3404, Nov. 2007.
[19] S. R. Cloude and E. Pottier, "A review of target decomposition theorems in radar polarimetry," *IEEE Trans. Geosci. Remote Sens.*, vol. 34, no. 2, pp. 498–518, Mar. 1996.
[20] A. Freeman and S. L. Durden, "A three-component scattering model for polarimetric SAR data," *IEEE Trans. Geosci. Remote Sens.*, vol. 36, no. 3, pp. 963–973, May 1998.
[21] E. Krogager, "New decomposition of the radar target scattering matrix," *Electron. Lett.*, vol. 26, no. 18, pp. 1525–1527, Aug. 1990.
[22] S. R. Cloude and E. Pottier, "An entropy based classification scheme for land applications of polarimetric SAR," *IEEE Trans. Geosci. Remote Sens.*, vol. 35, no. 1, pp. 68–78, Jan. 1997.
[23] J. S. Lee and E. Pottier, *Polarimetric Radar Imaging: From Basics to Applications*, 1st ed. Boca Raton, FL, USA: CRC Press, 2009.
[24] F. Berizzi, M. Martorella, A. Capria, R. Paladini, and D. Calugi, "H/α polarimetric features for man-made target classification," in *Proc. IEEE Radar Conf.*, Rome, Italy, May 2008, pp. 1–6.
[25] L. Guo, "Radar target HRRP polarimetric feature extraction and optimal selection," *Progr. Natural Sci.*, vol. 19, no. 7, pp. 784–792, Jul. 2009.
[26] L. Zhang, Y. Li, and Y. H. Wang, "Radar HRRP ground target recognition using slant 45° dual polarization," in *Proc. IEEE Radar Conf.*, Boston, MA, USA, Apr. 2019, pp. 1–5. doi: 10.1109/RADAR.2019.8835624.
[27] J. B. Keller, "Geometrical theory of diffraction," *J. Opt. Soc. Amer.*, vol. 52, no. 2, pp. 116–130, 1962.
[28] L. C. Potter and R. L. Moses, "Attributed scattering centers for SAR ATR," *IEEE Trans. Image Process.*, vol. 6, no. 1, pp. 79–91, Jan. 1997.
[29] M. J. Gerry, L. C. Potter, I. J. Gupta, and A. V. D. Merwe, "A parametric model for synthetic aperture radar measurements," *IEEE Trans. Antennas Propag.*, vol. 47, no. 7, pp. 1179–1188, Jul. 1999.
[30] E. F. Knott, J. F. Shaeffer, and M. T. Tuley, *Radar Cross Section*, Raleigh, NC, USA: SciTech Publishing, 2004.
[31] Y. C. Li and Y. Q. Jin, "Imaging and structural feature decomposition of a complex target using multi-aspect polarimetric scattering," *Sci. China Inf. Sci.*, vol. 59, no. 8, pp. 1–14, Aug. 2016. doi: 10.1007/s11432-015-5491-7.
[32] L. Du, P. Wang, H. Liu, M. Pan, F. Chen, and Z. Bao, "Bayesian spatiotemporal multitask learning for radar HRRP target recognition," *IEEE Trans. Signal Process.*, vol. 59, no. 7, pp. 3182–3196, Jul. 2011.
[33] G. Sinclair, "The transmission and reception of elliptically polarized waves," *Proc. IRE*, vol. 38, no. 2, pp. 148–151, Feb. 1950.
[34] J. Richards, A. Willsky, and J. Fisher, "Expectation-maximization approach to target model generation from multiple synthetic aperture radar images," *Opt. Eng.*, vol. 41, no. 1, pp. 150–166, Jan. 2002.
[35] W. L. Cameron, N. N. Youssef, and L. K. Leung, "Simulated polarimetric signatures of primitive geometrical shapes," *IEEE Trans. Geosci. Remote Sens.*, vol. 34, no. 3, pp. 793–803, May 1996.
[36] J. A. Jackson, B. D. Rigling, and R. L. Moses, "Canonical scattering feature models for 3D and bistatic SAR," *IEEE Trans. Aerosp. Electron. Syst.*, vol. 46, no. 2, pp. 525–541, Apr. 2010.
[37] S. R. Cloude, "Uniqueness of target decomposition theorems in radar rolarimetry," in *Direct Inverse Methods Radar Polarimetty* (NATO ASI Series), vol. 1. W. M. Boemer, Ed. Norwell, MA, USA: Kluwer, 1992, pp. 267–296.
[38] Y. Jiang, Y. Li, J. Cai, Y. Wang, and J. Xu, "Robust automatic target recognition via HRRP sequence based on scatterer matching," *Sensors*, vol. 18, no. 2, p. 593, Feb. 2018.
[39] H. Zhang, L. Xie, C. Wang, F. Wu, and B. Zhang, "Investigation of the capability of H-α decomposition of compact polarimetric SAR," *IEEE Geosci. Remote Sens. Lett.*, vol. 11, no. 4, pp. 868–872, Apr. 2014.
[40] W. L. Cameron and L. K. Leung, "Feature motivated polarization scattering matrix decomposition," in *Proc. IEEE IRC*, Arlington, TX, USA, May 1990, pp. 549–557.
[41] Y. Yu, C.-C. Chen, X. Feng, and C. Liu, "Modified entropy-based fully polarimetric target classification method for ground penetrating radars (GPR)," *IEEE J. Sel. Topics Appl. Earth Observat. Remote Sens.*, vol. 10, no. 10, pp. 4304–4312, Oct. 2017.
[42] W. Hong, "Hybrid-polarity architecture based polarimetric SAR: Principles and applications," *J. Radars*, vol. 5, no. 6, pp. 559–572, Dec. 2016.

TENG LONG (M'10–SM'13–F'18) was born in Fujian, China, in 1968. He received the M.S. and. Ph.D. degrees in electrical engineering from the Beijing Institute of Technology, in 1991 and 1995, respectively.

He was a Visiting Scholar with Stanford University, California, in 1999, and University College London, in 2002. He has been a Full Professor with the Department of Electrical Engineering, Beijing Institute of Technology, since 2000. He has authored or coauthored more than 300 articles. He has received many awards for his contributions to research and invention in China. His research interests include synthetic aperture radar systems and real-time digital signal processing, with applications to radar and communication systems. He is a Fellow of the Institute of Electronic and Technology and the Chinese Institute of Electronics.

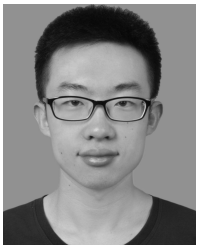

LIANG ZHANG was born in Nei Mongol, China, in 1993. He received the B.S. degree from the Beijing Institute of Technology, Beijing, China, in 2015, where he is currently pursuing the Ph.D. degree with the School of Information and Electronics. His current research interests include high resolution radar systems, radar polarimetric information processing, and radar automatic target recognition.

YANG LI was born in Liaoning, China. He received the B.S. degree in electrical engineering and the Ph.D. degree in target detection and recognition from the Beijing Institute of Technology, Beijing, China, in 2002 and 2007, respectively.

Since 2007, he has been a Lecturer with the School of Information and Electronics, Beijing Institute of Technology, where he has also been an Associate Professor, since October 2010. His research interests include high resolution radar systems and radar signal processing.

YANHUA WANG was born in Henan, China, in 1984. He received the B.S. degree in electrical engineering and the Ph.D. degree in target detection and recognition from the Beijing Institute of Technology, Beijing, China, in 2006 and 2011, respectively.

From March 2012 to October 2014, he was a Postdoctoral Research Associate with the Department of Electrical Engineering and Department of Biomedical Engineering, University at Buffalo, State University of New York, USA. Since 2014, he has been a Lecturer with the School of Information and Electronics, Beijing Institute of Technology, where he has also been an Associate Professor, since June 2019. His research interests include high resolution radar systems, signal processing, and radar automatic target recognition.